Proceedings of the 14th International Symposium on Process Systems Engineering – PSE 2021+
June 19-23, 2022, Kyoto, Japan

Primal-dual Feedback-optimizing Control with Direct Constraint Control

Risvan Dirza, Dinesh Krishnamoorthy, and Sigurd Skogestad*

Dept. of Chemical Engineering, Norwegian Univ. of Science & Technology (NTNU), NO-7491 Trondheim, Norway
**sigurd.skogestad@ntnu.no*

Abstract

This work proposes a strategy to track steady-state changes in active constraints and minimize dynamic constraint violations in order to achieve system-wide optimal operation using simple feedback control structures and logic blocks. The strategy is based on the recently proposed primal-dual feedback-optimizing control scheme that optimally handles steady-state changes in active constraints. However, the constraints are controlled in a slow time scale by updating the dual variables (Lagrange multipliers). To reduce dynamic constraint violations, we propose a "fix-up" to the primal-dual scheme with direct control of hard constraints. We show that the improved method can reduce profit loss in the long run by allowing for smaller back-off from hard constraints. The application is to coordinated control of gas-lifted oil wells.

Keywords: Distributed feedback-optimizing control, Oil/gas, Production optimization.

1. Introduction

The optimal process operation involves making decisions in real-time to meet production goals. This is typically done in the context of real-time optimization (RTO) using mathematical concepts, process models, and real-time measurements. In the 80s, there was an increasing interest in replacing model-based numerical solvers with a simple feedback loop, named feedback-optimizing control. The idea is to translate the economic objective into a process control objective by finding a function of the controlled variables (CVs), and when it is held constant, it leads to the optimal adjustment of the manipulated variables (MVs). These MVs drives the process to optimal operating condition (Morari et al., 1980). Twenty years later, Skogestad (2000) suggested replacing the term "optimal adjustments" with "acceptable adjustments" (in terms of the loss). This idea is known as self-optimizing control (SOC). In SOC, *"when the optimum lies at some constraints, we use active constraint control where the available MVs tightly control the constrained variables"*. When the optimum may be unconstrained, the self-optimizing CVs are measured variables or combinations of them. We need a good model to determine (offline) an accurate self-optimizing CV, and it can be time-consuming if we have a complex and large-scale system. Not considering noise, the ideal self-optimizing CV is the gradient of the cost function w.r.t. the control input, that when we keep at a constant setpoint of zero, it satisfies the necessary conditions of optimality (Halvorsen et al., 2003). In constrained cases, the process reaches ideal optimal operating conditions when the gradient of the Lagrange function w.r.t. to control input is kept at a constant setpoint of zero. If the objective function is additively separable, we can decompose the problem and let each local system controls its local gradients of the Lagrange function w.r.t. local control input. *In this framework, we need a central coordinator to update the shadow price of shared constraints and broadcast it to every subsystem (Wenzel et al., 2016).*

2. Recent Works and Problem Statement

Consider the following steady-state optimization problem of N different subsystems.

$$\min_{\mathbf{u}} J(\mathbf{u}, \mathbf{d}) = \sum_{i=1}^{N} J_i(\mathbf{u}_i, \mathbf{d}_i) \tag{1a}$$

$$s.t.\ \ \mathbf{g}_s(\mathbf{u}, \mathbf{d}) \leq \mathbf{0} \tag{1b}$$

where $\mathbf{u}_i \in \mathbb{R}^{n_{\mathbf{u}_i}}$ denotes the MVs for subsystem i, $n_{\mathbf{u}_i}$ is the number of MVs in subsystem i, and $\mathbf{u} = [\mathbf{u}_1 \quad \cdots \quad \mathbf{u}_N]^{\mathrm{T}}$, $\mathbf{d}_i \in \mathbb{R}^{n_{\mathbf{d}_i}}$ denotes the disturbances in subsystem i, $n_{\mathbf{d}_i}$ is the number of disturbances in subsystem i, and $\mathbf{d} = [\mathbf{d}_1 \quad \ldots \quad \mathbf{d}_N]^{\mathrm{T}}$, $J_i: \mathbb{R}^{n_{\mathbf{u}_i}} \times \mathbb{R}^{n_{\mathbf{d}_i}} \to \mathbb{R}$ is a function that denotes the local objective of subsystem i, $\mathbf{g_s}: \mathbb{R}^{n_\mathbf{u}} \times \mathbb{R}^{n_\mathbf{d}} \to \mathbb{R}^{n_{\mathbf{gs}}}$is a function that denotes the inequality (shared) constraints. $n_{\mathbf{g_s}}$ is the number of constraints. The Lagrangian function of problem (1) is $\mathcal{L}(\mathbf{u}, \mathbf{d}, \boldsymbol{\lambda}_{g,s}) = \sum_{i=1}^{N} J_i(\mathbf{u}_i, \mathbf{d}_i) + \boldsymbol{\lambda}_{g,s}^T \mathbf{g}_s(\mathbf{u}, \mathbf{d})$**,** where $\boldsymbol{\lambda}_{g,s} \in \mathbb{R}^{n_{\mathbf{gs}}}$ is the shadow price of the (shared) resource constraints. The goal of problem (1) is to determine optimal MVs to achieve system-wide steady-state optimal operation. Our motivation is to solve problem (1) using a feedback control structure that handles changing active constraints.

One possible approach is the reduced gradient approach or region-based control (Jäschke and Skogestad, 2012). *This method is easy to implement for a simple case with a few regions, and the result usually converges faster than the decomposed one for a large-scale problem. However, this method can be problematic for a complex and large case* as the number of the region is equal to $2^{n_{\mathbf{gs}}}$. Another attractive framework is distributed feedback-based real-time optimization, which is also known as primal-dual feedback-optimizing control (Dirza et al., 2021; Krishnamoorthy, 2021). This method can avoid solving numerical optimization problems online by having real-time iteration of dual/Lagrange decomposition (e.g., Wenzel et al. (2016)). Consequently, it has a central coordinator acting as a "slow" central constraint controller. This structure makes primal-dual flexible in the presence of changing active constraints. The problem with this method is that the constraint is controlled only on the slow time scale through the manipulation of the shadow prices, which is only indirectly through the unconstrained optimization layer that affects the (physical) MVs. This causes the shadow prices (broadcasted to the actual plant) to be suboptimal during the transient. This condition may lead to dynamic violation during the transient, and later lead to an infeasible operation. This violation is unacceptable when we have a hard constraint. Thus, it is necessary to introduce a "back-off" from that constraint. *Note that this back-off will also apply at a steady-state condition, and it may then result in a considerable economic penalty, which can lead to profit loss. This work addresses this violation issue and aims to minimize the profit loss.*

3. Proposed Control Structure

Mathematically, the profit loss scale is linear with the back-off parameter. One can express this as $Loss = -\boldsymbol{\lambda}_{g,s}{}^T \boldsymbol{\zeta}_{bo}$, where $\boldsymbol{\zeta}_{bo}$ is the back-off parameter, which means that by reducing the back-off parameter, one can reduce the profit loss in the long run.

Therefore, *this paper proposes an additional structure to control a hard constraint tightly in the primal-dual framework to minimize the back-off parameter*.

Because the primal-dual approach only has a central constraint controller that control the constraints on a slow time scale, we introduce direct constraint control as a ”fix-up” to reduce dynamic constraint violation. The direct constraint control is based on pairing the constraint with a particular MV using a selector. This tightly controls any active (shared-) hard constraints on a fast time scale. This structure automatically switches back to the unconstrained mode when none of those existing constraints turns active. *We introduce this proposed control structure as primal-dual feedback-optimizing control with direct constraint control*. The implementation is discussed in detail in Section 4 (see Fig. 2(b)).

Selectors, which are well-known tools in the industries, are used for active constraint switching (Krishnamoorthy and Skogestad, 2020). The switching determines the assigned value to the specified MV. When using selectors, only one of some control actions is the actual input to the plant at any given time. For the ones that are not selected, the feedback loop is “broken”. Consequently, the integral term is possibly building up. Thus, it is essential to implement anti-windup using a back-calculation scheme.

4. Implementation in Subsea Oil Production Network

We consider a subsea gas-lifted oil well production system, consisting of N clusters, that lift oil from the different reservoirs, completed with a fixed shared gas-lift compressor with limited available power. The production system model is like the one used in Dirza et al. (2021) and an additional model to calculate power consumption of the compressor as a linear function: $Pow_{gl} = \theta \sum_{i=1}^{N} \sum_{j=1}^{N_i} w_{gl,i,j}$, where θ is a function of a fixed ratio of outlet and inlet pressure of the compressor. Further, N_i is the total number of wells in cluster i, and $w_{gl,i,j}$ is the gas-lift rate injected to well j in cluster i.

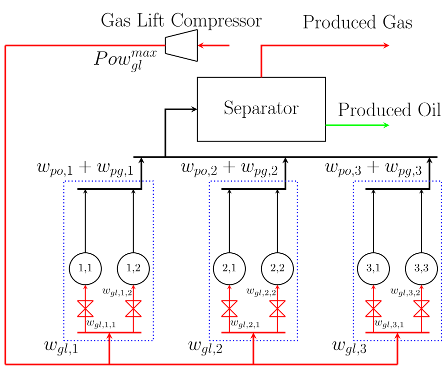

Figure 1: Field illustration

The objective function is to maximize the oil production income while minimizing the cost of the gas lift. The optimization problem is as follows.

$$\min_{\mathbf{w}_{gl}} \sum_{i=1}^{N} \left(-p_{o,i} \sum_{j=1}^{N_i} w_{po,i,j} + p_{gl,i} \sum_{j=1}^{N_i} w_{gl,i,j} \right) \tag{2a}$$

$$s.t.\ \ \mathbf{f}(\mathbf{x}, \mathbf{w}_{gl}, \mathbf{d}) = \mathbf{0} \tag{2b}$$

$$\mathbf{g}(\mathbf{x}, \mathbf{w}_{gl}, \mathbf{d}) \leq \mathbf{0} \tag{2c}$$

$$\mathbf{g}_s(\mathbf{x}, \mathbf{w}_{gl}, \mathbf{d}) = Pow_{gl} - Pow_{gl}^{max} \leq 0 \tag{2d}$$

where $p_{o,i}$, $p_{gl,i}$, and $w_{po,i,j}$ are the price of produced oil, the cost of gas-lift, and the produced oil rate of well j in cluster i, respectively. Pow_{gl} is the total power consumed by the fixed compressor to inject the total gas-lift rate i, and Pow_{gl}^{max} is the maximum available power, which can also be a function of back-off parameter, ζ_{bo}. Further, $\mathbf{x} \in$

$\mathbb{R}^{n_\mathbf{x}}$, and $\mathbf{d} \in \mathbb{R}^{n_\mathbf{d}}$ are the vectors of states, and disturbance (i.e., gas-oil-ratio) for the entire system. $\mathbf{w}_{gl} \in \mathbb{R}^{n_{\mathbf{w}_{gl}}}$ is the vector of inputs for the entire system, which can be seen as a vector of gas-lift rate from each well, $\mathbf{w}_{gl} = [w_{gl,1,1} \quad \cdots \quad w_{gl,N,N_N}]^\mathrm{T}$.

Constraint (2b) and (2c) represent model and physical constraints, respectively. We assume that one locally manages constraint (2c) to maintain the focus of the discussion. The objective function (2a) is additively separable. Moreover, Eq. (2d) is a linear and hard constraint. Thus, we can decompose the problem into N subproblems. This case study considers $N = 3$ subsea clusters, where each cluster has two production wells (see Fig. 1) and has different oil prices to indicate the type of oil produced by each reservoir is different.

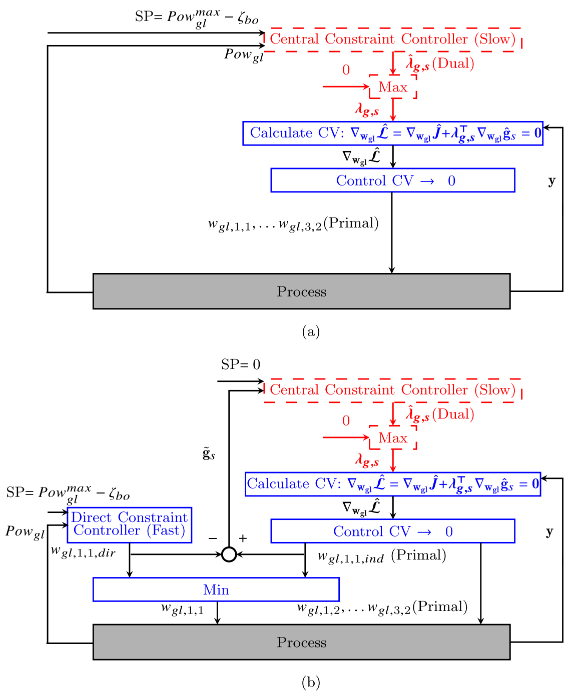

Figure 2: (a) Primal-dual control structure; (b) Proposed control structure which combines primal-dual optimization with direct constraint control.

As primal-dual can converge to optimal steady-state conditions (Dirza et al., 2021; Krishnamoorthy, 2021), *this simulation compares primal-dual (as shown in Fig. 2(a)) with the proposed control structures (as shown in Fig. 2(b)).* Note that $\mathbf{y}$ indicates the real-time measurements set. The grey boxes represent the physical system. The white boxes with solid blue lines represent a faster timescale computation block, and the white boxes with dashed red lines represent the slower ones.

Table 1: Controlled Variables, Setpoints, and Manipulated Variables

Well	CV	CV^{SP}	Calculated MV	Physical MV
1,1 (indirect)	$CV_{1,1,ind} = \nabla_{w_{gl,1,1}}\mathcal{L}_{1,1}$	0	$w_{gl,1,1,ind}$	$w_{gl,1,1}$
1,1 (direct)	$CV_{1,1,dir} = Pow_{gl}$	Pow_{gl}^{max}	$w_{gl,1,1,dir}$	$w_{gl,1,1}$
$\boldsymbol{i,j}^*$	$CV_{i,j,ind} = \nabla_{w_{gl,i,j}}\mathcal{L}_{i,j}$	0	$w_{gl,i,j,ind}$	$w_{gl,i,j}$

*: For the remaining well $\boldsymbol{j}$ in cluster $\boldsymbol{i}$

In the proposed control structure, we assume that well 1 of cluster 1 is technically more feasible to control hard constrained variables tightly. We have the original constraint $\mathbf{g}_s \leq 0$, and by using step response, we obtain that $\frac{d\mathbf{g}_s}{dw_{gl,11}} > 0$. This means that a small value of $w_{gl,1,1}$ is good in terms of satisfying the constraint and a min selector is needed,

$w_{gl,1,1} = min(w_{gl,1,1,dir}, w_{gl,1,1,ind})$, where $w_{gl,1,1,dir}$ is the MV computed by the direct constraint controller, and $w_{gl,1,1,ind}$ is the primal MV by the optimization block. Note that we, at the optimal steady-state, must have $w_{gl,1,1,dir} \geq w_{gl,1,1,ind}$ or equivalently $\tilde{\mathbf{g}}_s = w_{gl,1,1,ind} - w_{gl,1,1,dir} \leq \mathbf{0}$. This is the constraint controlled in the proposed new structure. Table 1 shows the CVs, Setpoints, and the MVs in this case study, where $\nabla_{w_{gl,i,j}}\mathcal{L}_{i,j} = \nabla_{w_{gl,i,j}}\boldsymbol{J} + \lambda_{\boldsymbol{g},\boldsymbol{s}}^T \nabla_{w_{gl,i,j}}\mathbf{g}_s$. Additionally, we use the same method as Dirza et al. (2021) to estimate steady-state cost and constraint gradient, labelled by $\nabla_{w_{gl,i,j}}\hat{\boldsymbol{J}}$ and $\nabla_{w_{gl,i,j}}\hat{\mathbf{g}}_s$, respectively.

The key idea is that we adjust the shadow price $\lambda_{g,s}$ so that on the long run the value of the MV computed by the direct constraint control (when it is active) is equal to the optimal primal value computed by the layer above (see Fig. 2(b)). To determine the applied $\lambda_{g,s}$, one can use a PI controller as a central constraint controller equipped with a max selector that gives 0 when the constraint is no longer active. The anti-windup is necessary to avoid $\lambda_{g,s}$ keeps changing in this case. Thus, this selector selects either 0 or the calculated shadow price $\hat{\lambda}_{g,s}$. Further, that shadow price $\hat{\lambda}_{g,s}$ at iteration k is as follows.

$$\hat{\lambda}_{g,s} = \lambda_{g,s}^k + K_p \tilde{\mathbf{g}}_s{}^k + \sum_{\tau=k-1}^{k} \left(K_I \tilde{\mathbf{g}}_s{}^\tau + K_{aw}\left(\lambda_{g,s} - \hat{\lambda}_{g,s}\right)^\tau\right) \tag{3}$$

where K_p, K_I, and K_{aw} are proportional, integral, and anti-wind-up gain, respectively.

PI controllers are tuned using the SIMC tuning method introduced by Skogestad (2003). The local controllers and the direct constraint controller have a sampling time of 1 sec. The central constraint controller updates the shadow price every 2.5 min because it may take more time to gather information from every cluster.

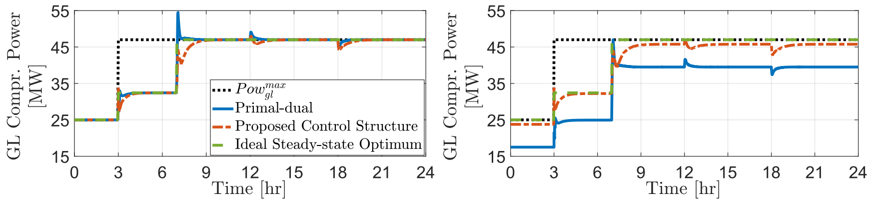

Figure 3: Left: Both Primal-dual and Proposed structure reach optimal steady-state conditions, but the constraint violation is much smaller for the proposed structure. Right: After implementing back-off from the power constraint.

Fig. 3 (left subplot) shows the simulation results when we consider $\zeta_{bo} = 0$. At time t = 3 hrs, the available power increases, and the shared constraint becomes inactive. Consequently, the gas-lift injection rates respond accordingly to achieve the optimal total available gas-lift allocation. Both primal-dual and proposed structure result in no dynamic violation at this time. At time t = 7 hrs, GOR dramatically decreases in all wells and causes extreme responses by the associated PI controllers. As a result, primal-dual significantly violates the constraint during the transient. We obtain a different result when applying the proposed control structure where Fig. 3 shows no dynamic constraint violation. At time t = 12 hrs, the GOR in most wells decreases, and the constraint is still active. The primal-dual has significant constraint violation during the transient for some time. As a comparison, the proposed structure responds accordingly and can reduce the magnitude and duration of that violation. At time t = 18 hrs, the GOR in most wells increases, and the constraint is still active. Both methods have no dynamic violation at this time. In general, the proposed structure can reduce those dynamic violations (in constrained cases) because (conceptually) direct constraint control selects the calculated direct constraint control input instead of the indirect one, which is calculated based on suboptimal shadow price during the transient.

In terms of dynamic violation magnitude, primal-dual and proposed structure can reach 7.4955 MW and 1.0329 MW, respectively. *When the maximum available power is a hard constraint, the proposed structure outperforms primal-dual as it can reduce more 'required' back-off, ζ_{bo} or even eliminate it (see Fig.3).* Fig. 4 shows the profit obtained by both methods in this simulation. The result indicates that the proposed one can reduce profit loss as much as 22,207.00 price unit *(0.18 %)* in 24 hours when one implements a back-off strategy for the same case and duration.

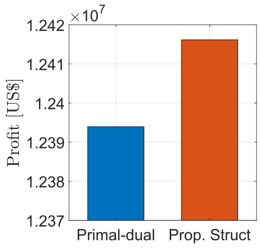

Figure 4: Profit $(-J)$ obtained by primal-dual and proposed structure in 24 hrs.

5. Conclusions

This work shows that the *proposed structure* with direct constraint control and primal-dual decomposition for optimization, is able to provide both tight constraint control on a fast timescale and optimal operation on a slow timescale. This strategy *offers* the possibility to reduce the back-off from constraints, which can give a large economic benefit.

6. Acknowledgment

The authors gratefully acknowledge the financial support from SUBPRO, financed by the Research Council of Norway, major industry partners, and NTNU.

References

R. Dirza, S. Skogestad, D. Krishnamoorthy, 2021. Optimal resource allocation using distributed feedback-based real-time optimization. IFAC-PapersOnLine 54 (3), 706–711, 16th IFAC Symposium on Advanced Control of Chemical Processes ADCHEM 2021.

I. J. Halvorsen, S. Skogestad, J. C. Morud, V. Alstad, 2003. Optimal selection of controlled variables. Industrial & Engineering Chemistry Research 42 (14), 3273–3284.

J. Jäschke, S. Skogestad, 2012. Optimal controlled variables for polynomial systems. Journal of Process Control 22 (1), 167–179.

D. Krishnamoorthy, 2021. A distributed feedback-based online process optimization framework for optimal resource sharing. Journal of Process Control (97), 72-83.

D. Krishnamoorthy, S. Skogestad, 2020. Systematic design of active constraint switching using selectors. Computers & Chemical Engineering 143, 107106.

M. Morari, Y. Arkun, G. Stephanopoulos, 1980. Studies in the synthesis of control structures for chemical processes: Part i: Formulation of the problem. process decomposition and the classification of the control tasks analysis of the optimizing control structures. AIChE Journal 26, 220 – 232.

S. Skogestad, 2000. Plantwide control: the search for the self-optimizing control structure. Journal of process control 10, 487 – 507.

S. Skogestad, 2003. Simple analytic rules for model reduction and pid controller tuning. Journal of Process Control 13, 291–309.

S.Wenzel, R. Paulen, G. Stojanovski, S. Kramer, B. Beisheim, S. Engell, 2016. Optimal resource allocation inindustrial complexes by distributed optimization and dynamic pricing. Automatisierungtechnik 64(6), 428–442.